

LQR State Estimator Coupled with Moore-Penrose Pseudoinverse H_∞ ESC Strategy: In-Wheel Motors driven Electric Vehicle co-simulation

Tommaso Favilli

*Department of Industrial Engineering
University of Florence
Florence, Italy
tommaso.favilli@unifi.it*

Margherita Montani

*Department of Industrial Engineering
University of Florence
Florence, Italy
margherita.montani@unifi.it*

Lorenzo Berzi

*Department of Industrial Engineering
University of Florence
Florence, Italy
lorenzo.berzi@unifi.it*

Renzo Capitani

*Department of Industrial Engineering
University of Florence
Florence, Italy
renzo.capitani@unifi.it*

Marco Pierini

*Department of Industrial Engineering
University of Florence
Florence, Italy
marco.pierini@unifi.it*

Luca Pugi

*Department of Industrial Engineering
University of Florence
Florence, Italy
luca.pugi@unifi.it*

Claudio Annicchiarico

*Meccanica42
Sesto Fiorentino (FI), Italy
claudio.annicchiarico@meccanica42.com*

Abstract—The availability of newly Electric Vehicle architectures equipped with independent In-Wheel-Motor traction layout, allows the improvement of lateral stability performances, by the development and the implementation of innovative torque allocation strategies. Indeed, enhanced handling properties during cornering manoeuvres could be achieved by an optimized braking and traction efforts dispatching algorithm to the wheels, especially when degraded adherence condition occurs in the tire-road contact interfaces. In this work, authors investigate the benefits achieved by a newly ESC lateral stability solution, based on Unscented Kalman Filtering with Linear Quadratic Regulator for yaw rate and sideslip angle estimations, integrated with Moore-Penrose pseudoinverse H_∞ wheel force allocation policy. The proposed strategy is coupled with longitudinal active safety systems. The assessment of the performances is done through co-simulation activities, imposing to the benchmark electric vehicle specific reference manoeuvres, in order to evaluate the achieved improvements from a stability and handling perspectives.

Index Terms—electric vehicle, in-wheel motor, lateral stability, LQR, H_∞ , stability control

I. INTRODUCTION

The transition of the current automotive market in the direction of road vehicle electrification [1], to meet stringent CO₂ emission requirements [2], is enhancing the development of advanced mechatronics and By-Wire (BW) system [3]–[5]. These solutions provide to designers and researchers numerous opportunity to reach higher lateral stability performances [6], [7] and functional safety level. Moreover, innovative Electric Vehicle (EV) architecture, e.g. Four Wheel Drive (4WD) layout with In-Wheel Motor (IWM), support the implementation of newly torque vectoring strategies, allowing each wheel to independently drive or brake [8]–[13]. So, it is evident that an appropriate design of braking/traction effort dispatch protocol appear as a feasible methodology to increase vehicle’s stability properties. This solutions could

effectively enhance handling vehicle’s characteristics, especially during cornering manoeuvres performed at poor adherence condition (e.g. wet/icy road pavement) or in scenario in which the imposed trajectory commits the maximum grip conditions of the tires [14].

The availability of Regenerative Braking System (RBS), however, require intensive efforts for the integration with conventional hydraulic plant, due to the over-actuated nature of the brake system [15]–[17]. This aspect, know as Brake Blending (BB), is essential to ensure the availability of minimum braking performances in every operative scenario. The synthesis of brake effort management strategy, as well as intrinsic advantages of proposed vehicle layout, could lead to remarkable leads from a reliability, functional safety and stability point of view [18]. The consequent increased complexity in the system architectures and the recent growing interest for IWM driven vehicle, requires the development of control strategies which combines the contribution of all the involved stability controllers. The synergetic coordination with different control structures need to be properly optimized.

Intent of the paper is to assess the possible improvement arising by an optimized coordination between proposed Electronic Stability Control (ESC) controllers with other stability regulators, i.e. Electronic Braking Distribution (EBD) and Anti-lock Braking System (ABS), in terms of vehicle’s dynamical behaviour, on a reference 4WD EV. The benchmark vehicle Use Case (UC) is a rear traction sport car. However, for the purpose of this study we suppose an alternative vehicle structure: a full traction layout with independent electric hub-motors equipped in each wheel. To fulfill these tasks, we decide to build a vehicle model following a co-simulation

approach between widely diffused simulation environments: *MATLAB Simulink* and *VI grade*. In this context, simulation campaign is carried out, making the EV perform specific reference manoeuvres, according to related standards.

II. AIM OF THE PAPER

Goal of the activity, which is an extension of the work developed in [19], concern the proposition of innovative torque regulation algorithms which can increase longitudinal and lateral stability performances, thanks to e-powertrains properties, challenging well-known and widely diffused wheel effort management policies. In particular, this work concerns the integration of proposed active stability controllers: EBD, ESC and ABS. Also, investigation of unconventional driveline architectures is performed in order to establish available improvements from a stability perspective. Respect to previously proposed work in literature, in this paper authors propose yaw rate and sideslip estimation algorithms based on Unscented Kalman Filter (UKF) Linear Quadratic Regulator (LQR) techniques [6], while torque allocation strategy rely on Moore-Penrose pseudoinverse H_∞ method [7], [20]. This solution aim at minimizing the difference between the driving performances requested by the pilot and the controllers, ensuring enhanced stable behaviour, fully exploiting IWM traction and braking characteristic.

The validation of the improvements achieved with the proposed architecture is performed with a model-based co-simulation approach in the *MATLAB Simulink* and *VI-Grade* environments. These models, developed using different modelling tools, are coupled using one platform as master and the other one as slave. In order to ensure no losses in the data exchange process during Real-Time (RT) simulation tests, a sample rates of 1 ms and a proper solvers are imposed.

This procedure allow the assessment of the performances permitted by the proposed control solution, observing dynamic and kinematic behaviour when imposing different open-loop reference manoeuvres to the EV, according to related standards. The obtained results were compared with those from a reference vehicle architecture: a conventional layout of the vehicle UC integrated with the ESC system [6].

III. ELECTRIC VEHICLE MODEL

The vehicle model, inspired by a real existing car, is a Rear Wheel Drive (RWD) vehicle configuration. However, we suppose a different powertrain layout, in order to investigate the performance improvements allowed by the proposed stability controllers: a 4WD architectures with IWMs, which independently actuate the EV wheels. Vehicle model consist of several sub-systems belonging to quite different physical domains (e.g. mechanical, electrical, electronic, controlling, and more). The main sub-models adopted for this work are:

- Driver Model: provide the drive command, i.e. brake and throttle demands (both dimensionless signals variable in the [0-1] range), along with the steer command.
- Stability Controller: developed ESC, EBD and ABS models are interposed between the driver and the Motor Control Unit (MCU) or the Brake Control Unit (BCU). Detailed characteristics of each controllers are explained in the dedicated sub-section.

- Electric Motor Model: composed by the MCU and the actuators, which reproduce the behaviour of a multi-quadrant operator IWM. The Electric Motor (EM) is controlled in order to trace the ideal power characteristic [1] and to work on multiple quadrants: the 1° during traction phases and the 4° during braking phases.
- Hydraulic Brake Plant Model: developed by Meccanica42 company, is composed by four electro-hydraulic units interposed between the main pump and the caliper of the brake system. Each unit is made by a controller and an electric motor, which command the hydraulic pump in order to deliver the target braking pressure to the wheel's caliper. They can be considered as a Controller Area Network (CAN) controlled device and so, can track a target pressure imposed by higher level control systems, thus simplifying the integration of the whole loop.
- Vehicle Model: implement dynamics and kinematics behaviours of the chassis, considering multiple Degree of Freedom (DOF), i.e. longitudinal, lateral and yaw motion. Also, account the interaction effects between tire and road, modelling the contact according to a Pacejka model [21].

The coupling between the *Vehicle Model* and the *Stability Controllers* is done according the block diagram scheme of Fig. 1.

A. Electronic Stability Program

ESC system is adopted to control the lateral behaviour of the vehicle's body during cornering manoeuvres. Using a reference vehicle model, the controller firstly calculate the expected yaw rate and sideslip angles, in function of the driver's inputs: front wheels steer angle and longitudinal speed. Then, compare these values with the ones that the vehicle is effectively experiencing, typically estimated through Inertial Measurement Unit (IMU) sensors platform and Artificial Neural Network (ANN)-UKF algorithm, as reported in [22]. If there is a not negligible error, evaluated with a proper dead-zone, the ESC apply torque vectoring control techniques to ensure the vehicle follows as close as possible the desired

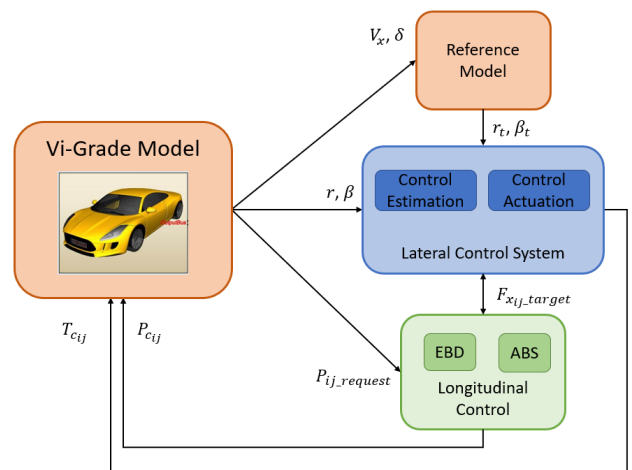


Fig. 1: Lateral Control Strategy Block Diagram

states (yaw rate and sideslip), delivering an equivalent yaw moment, according to the driver's command.

In conventional automotive solution, e.g. Internal Combustion Engine (ICE) vehicles, lateral stability strategies differentiates braking efforts between rights and lefts wheels, generating a correction yaw moment, in order to handling over-steering or under-steering conditions of the vehicle, typically occurring when turning in degraded adhesion scenario.

However, for the reference UC, lateral stability enhancement could be achieved thanks to IWM characteristics. Indeed, each actuator can both accelerate and decelerate, increasing the M_{yaw} that could be applied to the vehicle body. Assuming that we can separately control the torques exerted on every single wheel, is possible to improve ESC performances by allowing the single wheel also to traction, in addition to brake.

The proposed lateral control algorithm, shown in Fig.1, is composed by three sub-systems: the *Reference Dynamic Model*, the *Control Estimation System* and the *Control Command Actuation*.

1) *Reference Dynamic Model*: according to driver commands (steering wheel angle and pedals displacement) the vehicle body reference system vary with time. However, to underline inner vehicle characteristics (manoeuvrability) and control the under-steering/over-steering behaviour of the chassis, estimating the steady state values of the yaw rate (1) and sideslip angle (2) it's essential. These variables are expressed as a function of the *under-steering gradient* K , a coefficient depending from the vehicle wheelbase $a+b$, mass m and rear tires cornering stiffness C_y .

$$r_t = \frac{u}{(a+b) + u^2 K} \delta \quad (1)$$

$$\beta_t = \frac{b - \frac{m a u^2}{(a+b) C_{yf}}}{(a+b) + u^2 K} \delta \quad (2)$$

To ensure a stable behaviour of the vehicle during cornering manoeuvres, the ESC should control the available actuators in order to make the yaw rate r and the sideslip angle β strictly follow their optimal values, established from the *Reference Dynamic Model*. Nevertheless, expressions (1) and (2) doesn't accounts degraded adhesion conditions of the wheels, thus their values must be saturated to an upper threshold, depending on the available friction coefficient in the tire-road contact surface. In doing so, the reference model is implemented to provide the yaw rate and the sideslip angle references, once knowing the steering angle and the longitudinal speed, ensuring that the vehicle remains in grip and handling conditions.

2) *Control Estimation System*: the implemented ESC strategy is based on a LQR, an optimal control that is able to find, during driving scenario, the desired yaw torque which ensure stable behaviour of the chassis and passengers safety, as well as improved dynamic performances. Conventional LQR estimator works for a single linear dynamic model and are tuned specifically to reset the input variable [23]. The proposed LQR solution, as reported in [6], integrates a gain-scheduling control methodology, able to accurately follows the target value imposed by the *Reference Dynamic Model*, by adaptively tune itself in RT.

The states of the system are the actual yaw rate r and sideslip angle β , estimated by a single track vehicle model, and yaw rate r_t and nominal sideslip angle β_t arises from the reference model by solving (5), where A (3) and B (4) are the coefficients matrices.

$$A = - \begin{bmatrix} \frac{C_{yf} + C_{yr}}{m * vel_x} & \frac{1 + C_{yf} * a - C_{yr} * b}{m * vel_x^2} & 0 & 0 \\ \frac{C_{yf} * a - C_{yr} * b}{J} & \frac{C_{yf} * a^2 + C_{yr} * b^2}{J * vel_x} & 0 & 0 \\ 0 & 0 & \frac{1}{\tau_\beta} & 0 \\ 0 & 0 & 0 & \frac{1}{\tau_r} \end{bmatrix} \quad (3)$$

$$B = \begin{bmatrix} 0 \\ \frac{1}{J} \\ 0 \\ 0 \end{bmatrix} \quad (4)$$

$$\begin{Bmatrix} \dot{r} \\ \dot{\beta} \\ \dot{r}_t \\ \dot{\beta}_t \end{Bmatrix} = A \cdot \begin{Bmatrix} r \\ \beta \\ r_t \\ \beta_t \end{Bmatrix} + B \cdot \{M_y\} \quad (5)$$

In (5) the dynamic states evolution is expressed by vehicle geometric parameters, i.e., the front and rear wheelbase a and b , the vehicle mass m and yaw moment of inertia J , the front and rear cornering stiffness, C_{yf} and C_{yr} respectively, and the longitudinal vehicle speed, which is scheduled at intervals of 10 m/s.

Defining the output of the controller as the difference between reference and actual states, it's possible to establish the optimal controller gains. This allow to correctly determine the control signal: an equivalent yaw moment M_{yaw} , which is delivered to the vehicle body by the EM and by the hydraulic brake plant (6).

$$\begin{Bmatrix} \delta_c \\ M_{yaw} \end{Bmatrix} = \begin{bmatrix} K_{\delta r} & K_{\delta \beta} & K_{\delta r t} & K_{\delta \beta t} \\ K_{M r} & K_{M \beta} & K_{M r t} & K_{M \beta t} \end{bmatrix} * \begin{Bmatrix} r \\ \beta \\ r_t \\ \beta_t \end{Bmatrix} \quad (6)$$

To be implemented in Real-Time, all the control logic is discretized with a sample time of 0,001 s.

3) *Control Command Actuation*: the optimal allocation strategy proposed here is based on the Moore-Penrose pseudoinverse [7]. We would like to accomplish two different tasks: 1) ensure a desired stable lateral behaviour of the vehicle and 2) produce a minimum correction moment, which must be also in accordance with the driver intent. The followed approach appear efficient, since minimize the norm 2 of the functional cost (7), which attempt to stabilize the vehicle lateral behaviour, while minimizing the correction efforts.

$$\|T_{cmd-k} - T_{cmd-k}^*\|_2 = \left(\sum_{k=1}^{n=4} (T_{cmd-k} - T_{cmd-k}^*)^2 \right)^{1/2} \quad (7)$$

where $k \in \{fl, fr, rl, rr\}$ indicate the wheel (front left, front right, rear left, rear right), y_k is the half-track of the corresponding wheel, R_w the tire radius, T_{cmd-k} and T_{cmd-k}^* are the torques requested by the driver and by the ESC controller, respectively.

The reference wheel torques is given by (8).

$$\begin{bmatrix} \frac{-y_{fl}}{R_w} & \frac{y_{fr}}{R_w} & \frac{-y_{rl}}{R_w} & \frac{y_{rr}}{R_w} \\ 1 & 1 & 1 & 1 \end{bmatrix} \begin{bmatrix} T_{cmd-fl} - T_{cmd-fl}^* \\ T_{cmd-fr} - T_{cmd-fr}^* \\ T_{cmd-rl} - T_{cmd-rl}^* \\ T_{cmd-rr} - T_{cmd-rr}^* \end{bmatrix} = \begin{bmatrix} M_{yaw} \\ 0 \end{bmatrix} \quad (8)$$

As can be seen, the first row correspond to the task 1), while the second row reflect the task 2). The resolution of (8) occur in four sequential steps. In each k -th step the value of T_{cmd-k}^* is checked respect to its upper and lower constrain limits. If it exceeds them, is subsequently saturated at this value. At the $(k+1)$ -th steps (8) is recalculated, excluding from the system the row related to the k -th torque reference, assumed equal to its own limitations.

The algorithm is parameterized respect to the wheels torque constrains, in order to guarantee maximum flexibility and portability of the code respect to different vehicle architectures. This ensure that the requested torques are in accordance with the actuators limitations, allowing, in addition, the implementability of advanced torque vectoring techniques. Is the case of the benchmark vehicle investigated in this paper, in which positive and negative efforts could be delivered independently on each wheel, even of the same axis.

B. Electronic Braking Distribution

The EBD is a control unit widely adopted in the automotive field, used to privilege braking performances of the vehicle's axes, in function of front/rear longitudinal load transfer. According to [24], the set of optimal points, as the adhesion coefficient in the tire-road interface changes, is a parabola, visible in Fig. 2(1). This curve is calculated by solving (9), where F_{ij} is the wheel force, with the subscript $i \in \{x, y, z\}$ for longitudinal, lateral and vertical respectively, while $j \in \{f, r\}$ for front and rear axle, the superscript 0 indicate stationary conditions, μ the friction coefficient, h the vertical distance between vehicle Centre Of Gravity (COG) and the ground, l the wheelbase.

$$F_{zf} = \frac{F_{xf}}{\mu} = F_{zf}^0 + \frac{h}{l}(F_{xf} + F_{xr}) \quad (9)$$

The curve define the load distribution coefficients between the axes which, for the specified friction coefficient,

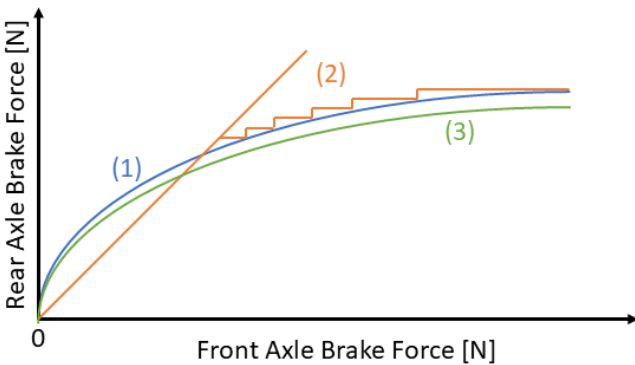


Fig. 2: Front/Rear Axle Braking Force EBD distribution: (1) Ideal; (2) Conventional; (3) Proposed.

maximize the available deceleration while avoiding wheels sliding. Typically, conventional EBD controller approximate this function with a simple ramp which apply a 50/50 ratio axle braking, leaving to the ABS controller the burden to avoid rear wheels sliding (Fig. 2(2)).

Use more conservative strategy could reduce the onset of wheel slippage, but underestimate the available deceleration performances, not allowing to completely exploit the braking actuators and minimize the stopping distance for degraded friction conditions. However, the new architecture of by-wire system allows to reduce the delay respect to the one in modern EV, thanks to the positioning of the hydraulic component close to the wheel. The use of four independent actuators ensures to obtain the optimal brake distribution and increases system safety. In order to compensate the uncertainty of the adhesion coefficient we adopt a parabola which slightly deviate from the ideal curve (Fig. 2(3)). In this way the front/rear braking allocation strategy appear more robust respect to error in the friction value estimation, resulting in quite reliable exploitation of available friction coefficient.

C. Anti-Lock Braking System

To ensure the stability during braking actuation and improve the handling and controllability of the vehicle, both in longitudinal and cornering manoeuvres, an ABS is recommended (Fig.1). It is implemented a proportional integral derivative (PID) controller that allows to follow the target longitudinal wheel slip [25]. The PID output is the single pressure which, if applied on every wheel, reduce the error between target and actual value of the slip s shown in Fig. 3. In this way it is possible to avoid the wheels locking when braking, reducing the corresponding stopping distance and the under/over-steer behavior of vehicle in cornering scenario, ensuring a stable behaviour in accordance to the driver steer input.

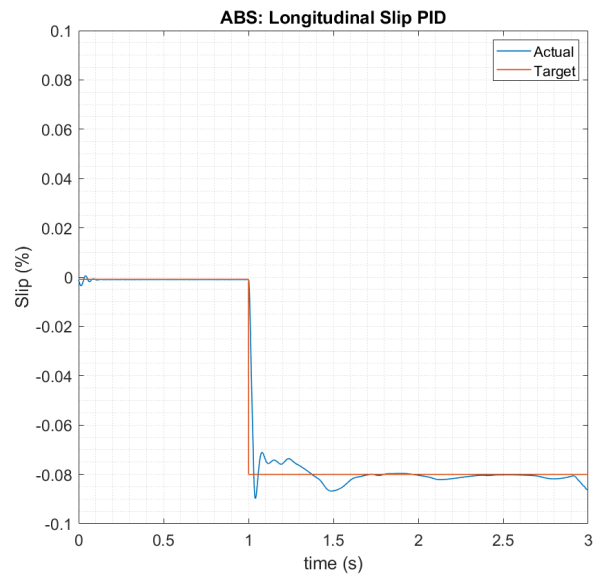


Fig. 3: Longitudinal wheel slip during full braking with ABS operation.

The target wheel slip is calculated from the desired longitudinal force, arising from the EBD in case of brake pedal actuation, or from the ESC system. Knowing the longitudinal front and rear stiffness of the tires and assuming a linear behaviour of the latter, target longitudinal slip is calculated through (10).

$$\sigma_t = \frac{F_x}{C_x} \quad (10)$$

This value is saturated from zero, so that the control only works when braking, to near -0.1, ensuring that the wheel maintain itself in the linear dynamic range.

Instead the actual value of the longitudinal slip is estimated by (11).

$$\sigma = \frac{V_x - \omega * R_w}{V_x} \quad (11)$$

Compared to traditional ABS on-off control system, due to the brake architecture adopted in this context, proposed controller ensures smooth braking behavior improving driver comfort as it's shown on the output of performed tests.

IV. SIMULATION CAMPAIGN RESULTS

To evaluate the stability performances improvement allowed by the controllers, we make the vehicle perform specific reference manoeuvres and compare the results obtained with the ones of the UC vehicle equipped with only the ESC and ABS, without any integration logic. Simulation tests on the proposed EV model, implemented in the co-simulation environment of *MATLAB Simulink* and *VI Grade*, could be grouped in two branch: *Longitudinal Stability tests*, useful for the assessment of EBD and ABS effects on the braking distance; *Lateral Stability tests*, executed to understand the impact of the ESC system on the vehicle lateral behaviour.

A. Longitudinal Stability Test

Consist in the execution of straight-line deceleration for several friction coefficient values. Indeed, for degraded tire-road adhesion conditions, EBD and ABS controller are essential to ensure the minimum braking performances required by the ISO21994 standards [26], reducing the corresponding vehicle braking distance. Results are showed in Fig. 4 and summarized in Table I for the vehicle UC.

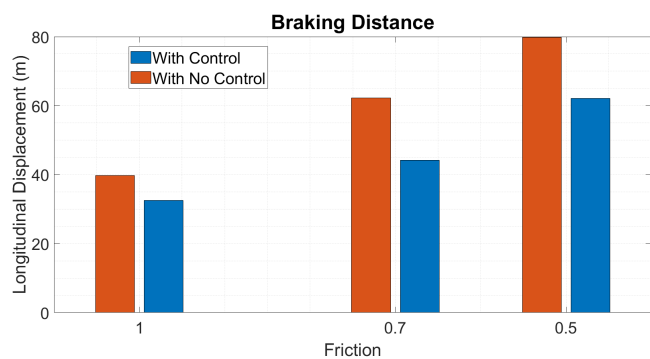


Fig. 4: Vehicle braking distance in longitudinal braking maneuver in accordance to ISO21994 standard specification and a friction coefficient of: 1, 0.7 and 0.5, supposing availability and unavailability of the ABS control system.

TABLE I: Stopping Distance of the Longitudinal Stability Tests for Different Adherence Conditions

Initial Speed: $V_{x,i}=27.78$ [m/s]			
Adherence μ [0-1]	ABS	Stopping Dist. [m]	Improvement [%]
1	ON	32.56	18.13%
	OFF	39.77	
0.7	ON	44.14	29.02%
	OFF	62.19	
0.5	ON	62.12	22.17%
	OFF	79.82	

Current regulations recommend that the stopping distance, during longitudinal braking scenario, must remain under 40 meters for nominal friction values and an initial vehicle speed of 100 km/h. Output are obtained supposing alternatively the availability and unavailability of the ABS controller, to highlight its contribution on the stopping distance reduction, showing also the corresponding improvement in terms of distance percentage. In addition, in Fig. 5 the wheels' and vehicle speed are shown, to underline the avoidance of wheel locking and the driver comfort improvement with the ABS implemented, compared with the conventional bang-bang wheels acceleration controller.

B. Lateral Stability Test

These simulations campaign are executed in order to asses the effect of the proposed ESC algorithm on lateral stability performances and highlight the improvements, compared with results related to the control structure described in [6]. Two different tests are executed: the *Double Lane Change (DLC)* [27] and the *Sine With Dwell* tests [28].

For the DLC, tests are repeated increasing the reference speed, until the vehicle is able to correctly perform the trajectory, supposing availability and unavailability of the proposed controlling method. The improvement are evaluated observing the maximum speed at which the vehicle executes the imposed steering manoeuvres without leaving the admitted zone and hitting the corners (Fig. 6). This figure shows how the vehicle equipped by the proposed control is able to perform the manoeuvre at 60 km/h. Instead, vehicle with only standard ESC, i.e. excluding the Moore-Penrose pseudoinverse from the control algorithm, is unable to fulfill test requirements at the same speed. In addition, in Fig. 7 the comparison of the speed during DLC manoeuvre for the investigated UCs, shows a lesser vehicle speed reduction in the second phase of the trajectory and a faster return to target speed, due to a better distribution of the vehicle torque values, visible in Fig. 8. The braking pressure (SubFig. 8a) are lower in some cases and the traction torques (SubFig. 8b) are distributed on the four wheels.

The performances evaluation of the ESC during the Sine with Dwell manoeuvre (open-loop test) is done evaluating two key parameters: the sideslip angle β and the yaw rate r . This test consist of a maneuver, performed at 80 km/h, in which the steering wheel angle is linearly increased until to a lateral acceleration of 0.3 g is reached. Then, the steer angle must follow a sine function at 0.7 Hz frequency, while the amplitude depend of the value established at the stage before.

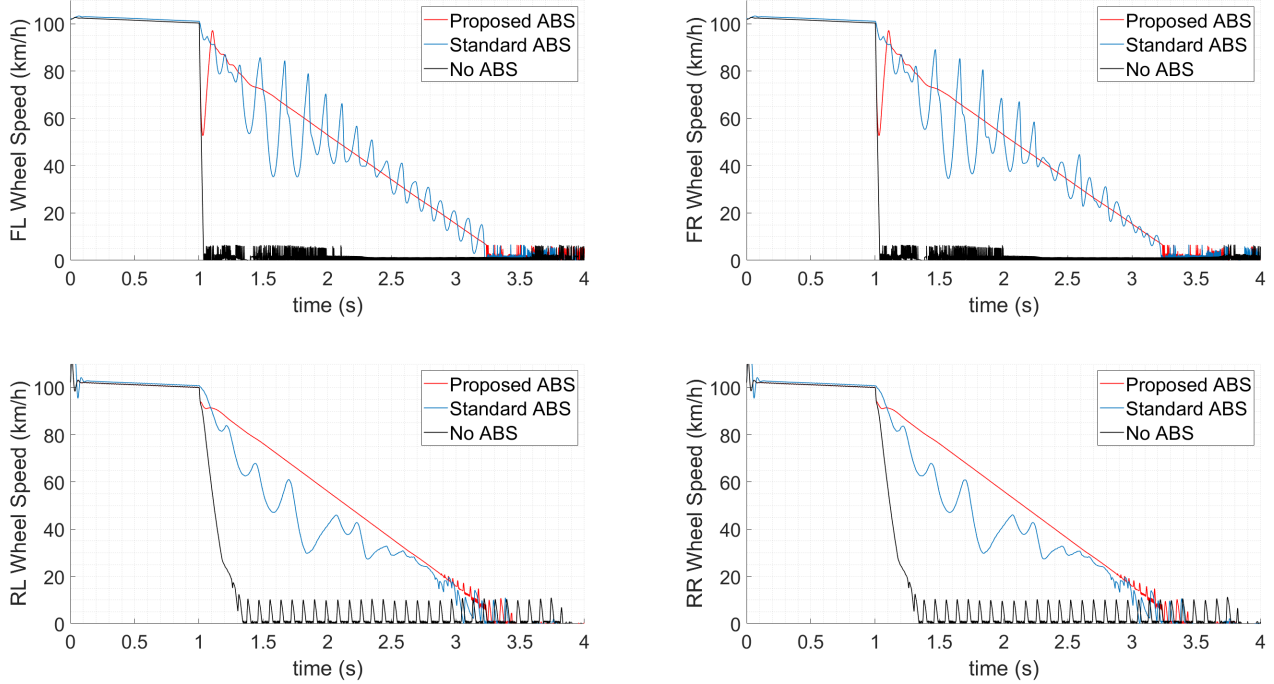


Fig. 5: Vehicle wheels speed in longitudinal braking maneuver in accordance to ISO21994 standard specification, supposing availability and unavailability of the proposed ABS control system and a standard on-off controller on the wheels acceleration.

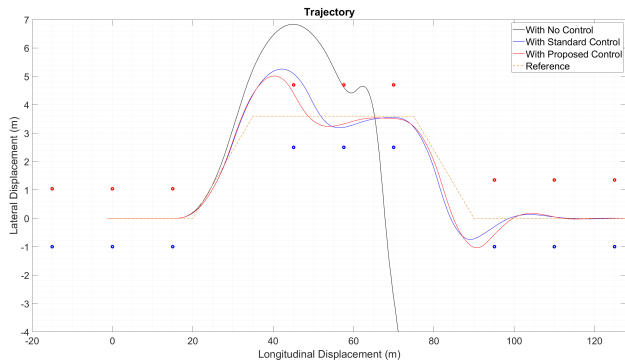


Fig. 6: Vehicle trajectory in a Double Lane Change maneuver, with a longitudinal speed of 60 km/h and a friction of 1, supposing availability and unavailability of the ESC control systems.

The test is assumed accomplished if the yaw rate of the vehicle returns to zero in a time less than T_0 (the time required to the steer angle to reach its reference) plus 1.75 s. Fig. 9 shows the target and actual values of yaw rate and sideslip angle. Plots display the behaviour the vehicle is experiencing, supposing availability and unavailability of the controller, and the performance of the ESC without Moore-Penrose pseudoinverse integration logic.

In Fig. 11 is visible that the stability is reached at higher vehicle speed, ensuring an improved integration between control and driver inputs (Fig.10).

The assumption to alternatively suppose availability and unavailability of the stability controller is done in order to comparatively assess the simulation outputs of the performed tests. In particular, the results of the tests in which the controller systems are disabled are assumed as a reference baseline for the metrical evaluation of the obtained improvements. Instead, the assumption to compare the proposed control architecture with a one without an integration logic is used to show how this new structure improves the performance, as well as ensures the driver intent with the aim of providing stability, comfort and smoothness.

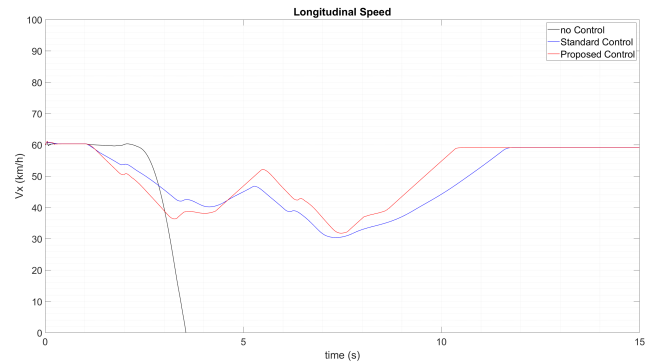
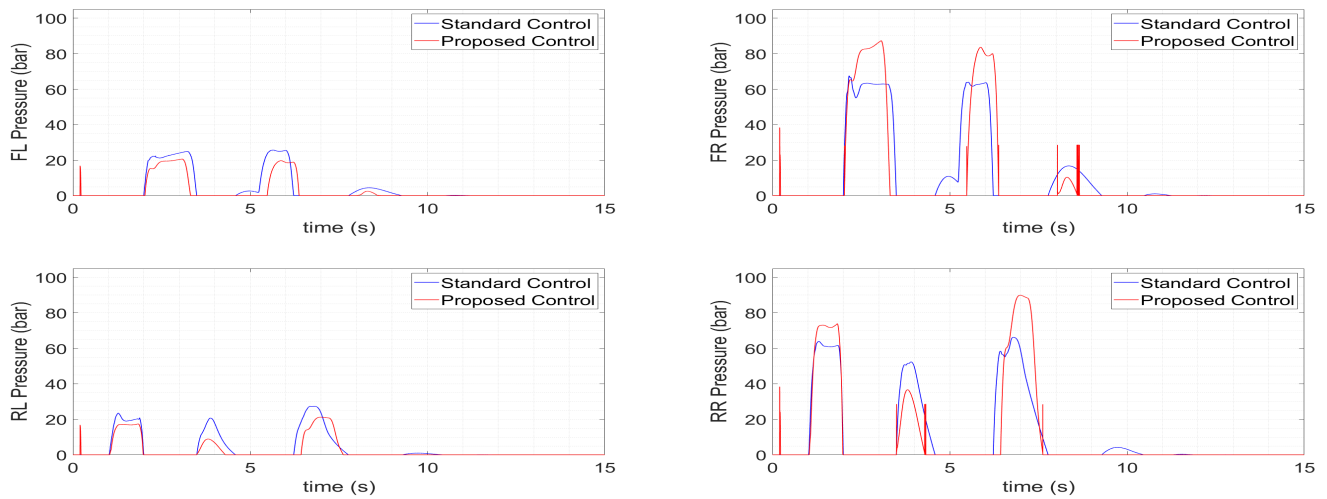
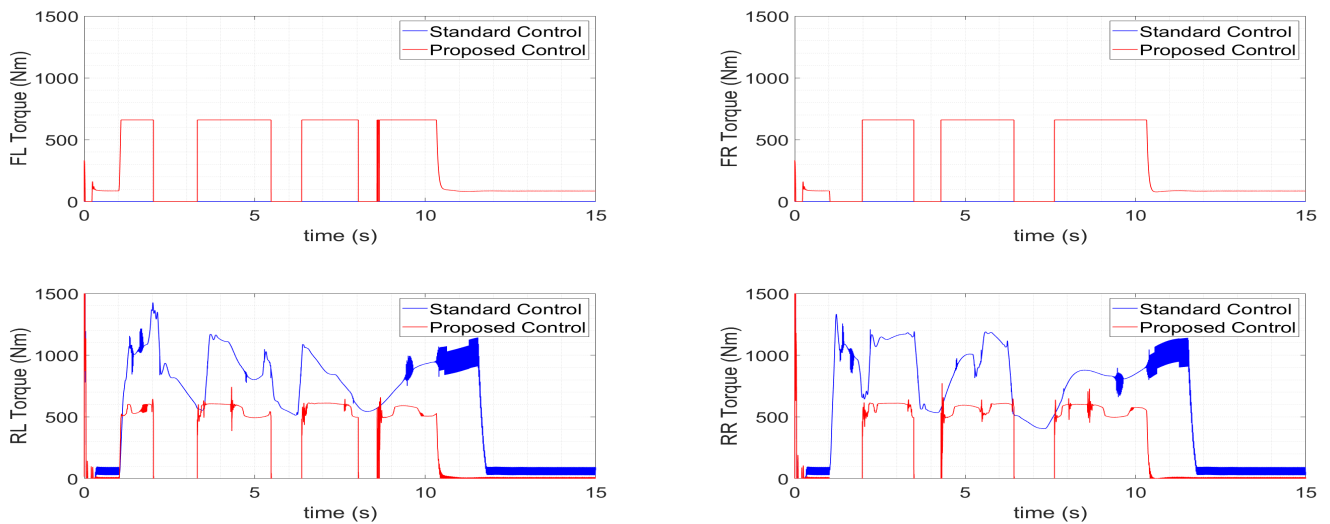


Fig. 7: Vehicle Longitudinal speed during Double Lane Change maneuver, with a longitudinal speed of 60 km/h and a friction of 1, supposing availability and unavailability of the ESC control systems.



(a) Brake Pressures



(b) Driving Moments

Fig. 8: Braking and driving torque vehicle inputs comparing Standard and Proposed architecture control performances.

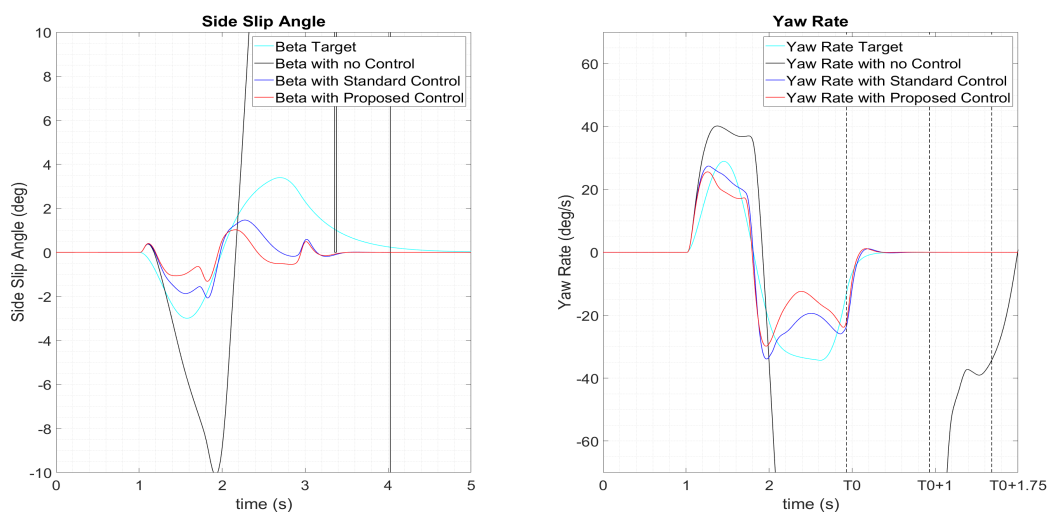


Fig. 9: Target and effective vehicle sideslip angle β and yaw rate r during Sine With Dwell maneuver, with a longitudinal speed of 80 km/h and a steering wheel angle of 270 deg, supposing availability and unavailability of the ESC control systems.

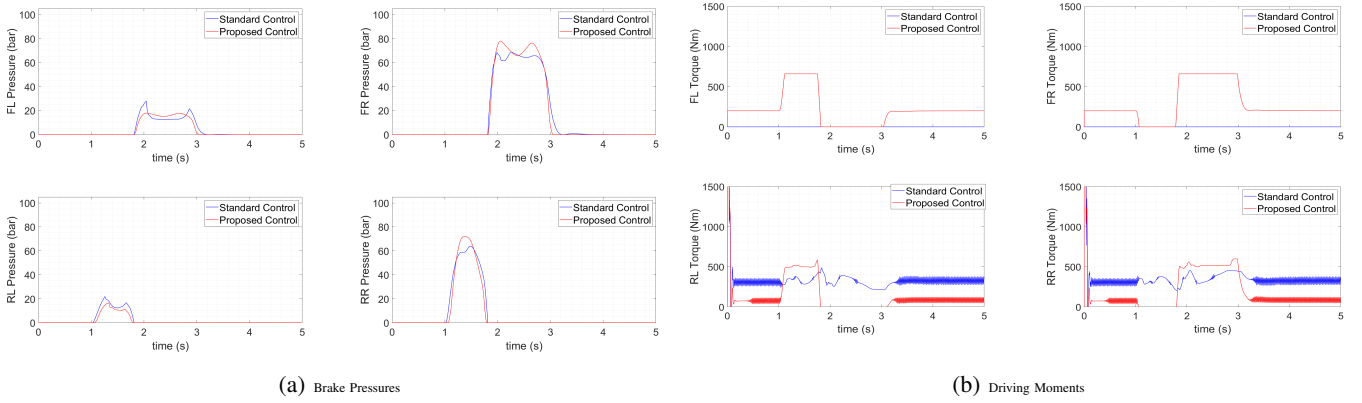


Fig. 10: Braking and driving torque vehicle inputs comparing Standard and Proposed architecture control performances.

V. CONCLUSIONS AND FUTURE DEVELOPMENTS

Most interesting output of the performed simulation tests campaign concern the dynamical vehicle behaviour improvements allowed by the proposed controllers, both respect to longitudinal and lateral stability. Result arise from a model-based implementation of the investigated EV in a co-simulation environment, involving MATLAB Simulink and VI Grade.

Assessment of the longitudinal stability enhancement is done in accordance to [26], evaluating the stopping distance of the vehicle, assuming fixed boundary condition. Result of Fig. 4 and Table I suggest that the ABS controller is fundamental to ensure a safe behaviour during straight line deceleration. Instead, Fig. 5 indicates that the proposed ABS strategy, based on PID control logic of the longitudinal slip, makes effective and smoothness the braking effort respect a on-off control on the wheel acceleration. Indeed, for different adherence conditions, the Anti-slip strategy appear effective, since reduce the corresponding longitudinal distance between the starting of the brake manoeuvres and the completely stopping of the vehicle, if compared with the case in which ABS controller is disabled. It's interesting to note also that, for normal adherence conditions, the adopted policy successfully fulfills the limitations imposed by the mandatory standards.

For the lateral stability, we investigate the performance improvements by observing the result of DLC [27] and Sine with D-well tests [28]. Concerning the Double-Lane Change, it can be stated that, looking at the outputs of Fig. 6 and Table II, the proposed ESC strategy can ensure a stable lateral behaviour of the vehicle, by increasing the speed at which the

TABLE II: Maximum Vehicle Speed During Double Lane Change Tests for Different Adherence Conditions

Double-Lane Change			
Adherence μ [0-1]	ESP	Max. Speed [km/h]	RSME
1	ON	60	0.52
	OFF	40	0.78
0.7	ON	45	0.40
	OFF	30	0.53
0.5	ON	35	0.11
	OFF	30	0.28

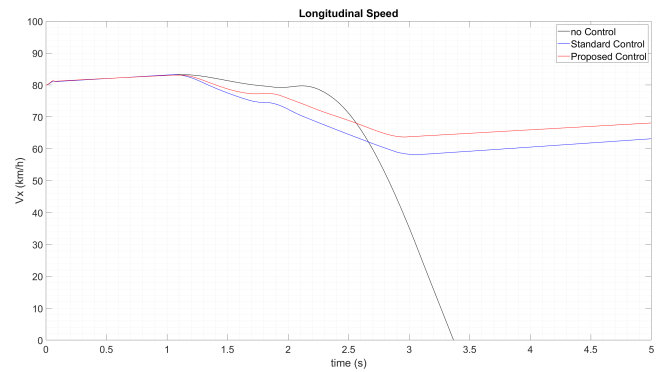


Fig. 11: Vehicle Longitudinal speed during Sine With Dwell maneuver, with a longitudinal speed of 80 km/h and a steering wheel angle of 270 deg, supposing availability and unavailability of the ESC control systems.

reference trajectory could be executed and by reducing the Root Square Mean Error (RSME) respect to the ideal curve of the manoeuvre (centered respect to the admitted zone). Results of the Sine with Dwell tests are visible in Fig. 9. The plots clearly show that the ESC controller increase the stability performances, reducing the error between target and real value of β and r during the execution of the imposed manoeuvre.

Fig. 7, Fig. 8, Fig. 9, Fig. 10 and Fig. 11 show how the Moon-Penrose pseudoinverse torque allocation strategy is able of ensuring desired yaw moment, calculated from the LQR filter implemented in the ESC state estimator, integrated with the pedal and steer driver demands. In this way, it's possible to provide stability, safety and passengers comfort.

Summarizing, we can conclude by saying that, in this work, the proposed longitudinal stability controllers, i.e. EBD and ABS, are correctly integrated with the lateral stability controller ESC, based on LQR yaw moment/sideslip estimator and Moore-Penrose torque allocation strategy, in order to accomplish enhanced stability behaviours of the IWM driven e-vehicle, if compared with conventional activate safety controllers.

Possible future developments concerns the further refining of the vehicle models and sub-models, in order to faithfully replicate real driving scenario conditions, along with a better

tuning of the controller parameters, aiming at increasing the stability performances. Also, a gain-scheduling controlling method for the ESC is planned, coupled with friction coefficient estimation system, to adjust controller robustness respect to adherence variation in tire-road interfaces.

REFERENCES

- [1] J. de Santiago et al., 'Electrical Motor Drivelines in Commercial All-Electric Vehicles: A Review', *IEEE Transactions on Vehicular Technology*, vol. 61, no. 2, pp. 475–484, Feb. 2012, doi: 10.1109/TVT.2011.2177873.
- [2] European Parliament, Council of the European Union, Regulation (EC) No 715/2007 of the European Parliament and of the Council of 20 June 2007 on type approval of motor vehicles with respect to emissions from light passenger and commercial vehicles (Euro 5 and Euro 6).
- [3] L. Yu, X. Liu, Z. Xie, and Y. Chen, 'Review of Brake-by-Wire System Used in Modern Passenger Car', in Volume 3: 18th International Conference on Advanced Vehicle Technologies; 13th International Conference on Design Education; 9th Frontiers in Biomedical Devices, Charlotte, North Carolina, USA, Aug. 2016, p. V003T01A020, doi: 10.1115/DETC2016-59279.
- [4] N. Kyura and H. Oho, 'Mechatronics-an industrial perspective', *IEEE/ASME Trans. Mechatron.*, vol. 1, no. 1, pp. 10–15, Mar. 1996, doi: 10.1109/3516.491405.
- [5] L. Berzi, T. Favilli, E. Locorotondo, M. Pierini, and L. Pugi, 'Real Time Models of Automotive Mechatronics Systems: Verifications on "Toy Models"', in *Advances in Italian Mechanism Science*, vol. 68, G. Carbone and A. Gasparetto, Eds. Cham: Springer International Publishing, 2019, pp. 141–148.
- [6] M. Montani, R. Capitani, M. Fainello, and C. Annicchiarico, 'Use of a driving simulator to develop a brake-by-wire system designed for electric vehicles and car stability controls', in 10th International Munich Chassis Symposium 2019, P. E. Pfeffer, Ed. Wiesbaden: Springer Fachmedien Wiesbaden, 2020, pp. 663–684, doi: 10.1007/978-3-658-26435-246.
- [7] L. Pugi, T. Favilli, L. Berzi, E. Locorotondo, and M. Pierini, 'Brake Blending and Optimal Torque Allocation Strategies for Innovative Electric Powertrains', in *Applications in Electronics Pervading Industry, Environment and Society*, vol. 573, S. Saponara and A. De Gloria, Eds. Cham: Springer International Publishing, 2019, pp. 477–483.
- [8] R. de Castro, M. Tanelli, R. E. Araújo, and S. M. Savaresi, 'Minimum-time manoeuvring in electric vehicles with four wheel-individual-motors', *Vehicle System Dynamics*, vol. 52, no. 6, pp. 824–846, Jun. 2014, doi: 10.1080/00423114.2014.902973.
- [9] C. Feng, N. Ding, Y. He, G. Xu, and F. Gao, 'Control allocation algorithm for over-actuated electric vehicles', *J. Cent. South Univ.*, vol. 21, no. 10, pp. 3705–3712, Oct. 2014, doi: 10.1007/s11771-014-2354-0.
- [10] K. Sung-Yeon, K. Ji-Weon, L. Sang-Moon, C. Jae-Seung, and K. Hyun-soo, 'A Study on In-wheel Motor Control to Improve Vehicle Stability Using Human-in-the-Loop Simulation', *Journal of Power Electronics*, vol. 13, no. 4, pp. 536–545, Jul. 2013, doi: 10.6113/JPE.2013.13.4.536.
- [11] Kanghyun Nam, H. Fujimoto, and Y. Hori, 'Lateral Stability Control of In-Wheel-Motor-Driven Electric Vehicles Based on Sideslip Angle Estimation Using Lateral Tire Force Sensors', *IEEE Trans. Veh. Technol.*, vol. 61, no. 5, pp. 1972–1985, 2012, doi: 10.1109/TVT.2012.2191627.
- [12] B. Jin, C. Sun, and X. Zhang, 'Research on Lateral Stability of Four Hubmotor- In-Wheels Drive Electric Vehicle', *International Journal on Smart Sensing and Intelligent Systems*, vol. 8, no. 3, pp. 1855–1875, 2015, doi: 10.21307/ijssis-2017-833.
- [13] L. Pugi, F. Grasso, M. Pratesi, M. Cipriani, and A. Bartolomei, 'Design and preliminary performance evaluation of a four wheeled vehicle with degraded adhesion conditions', *IJEHV*, vol. 9, no. 1, p. 1, 2017, doi: 10.1504/IJEHV.2017.082812.
- [14] M. Montani et al., 'ESC on In-Wheel Motors Driven Electric Vehicle: Handling and Stability Performances Assessment', in 2020 IEEE International Conference on Environment and Electrical Engineering and 2020 IEEE Industrial and Commercial Power Systems Europe (EEEIC / ICPS Europe), Madrid, Spain, Jun. 2020, pp. 1–6, doi: 10.1109/EEEIC/ICPSEurope49358.2020.9160768.
- [15] C. Lv, J. Zhang, Y. Li, and Y. Yuan, 'Regenerative Braking Control Algorithm for an Electrified Vehicle Equipped with a By-Wire Brake System', presented at the SAE 2014 World Congress Exhibition, 2014, pp. 2014-01–1791, doi: 10.4271/2014-01-1791.
- [16] L. Berzi et al., 'Brake Blending Strategy on Electric Vehicle Co-simulation Between MATLAB Simulink® and Simcenter Amesim™', in 2019 IEEE 5th International forum on Research and Technology for Society and Industry (RTSI), Florence, Italy, 2019, pp. 308–313, doi: 10.1109/RTSI.2019.8895548.
- [17] L. Pugi, T. Favilli, L. Berzi, E. Locorotondo, and M. Pierini, 'Application of Regenerative Braking on Electric Vehicles', in 2019 IEEE International Conference on Environment and Electrical Engineering and 2019 IEEE Industrial and Commercial Power Systems Europe (EEEIC / ICPS Europe), Genova, Italy, 2019, pp. 1–6, doi: 10.1109/EEEIC.2019.8783318.
- [18] T. Favilli, L. Pugi, L. Berzi, M. Pierini, and N. Tobia, 'Regenerative Fuzzy Brake Blending Strategy on Benchmark Electric Vehicle: the FIAT 500e', in 2020 IEEE International Conference on Environment and Electrical Engineering and 2020 IEEE Industrial and Commercial Power Systems Europe (EEEIC / ICPS Europe), Madrid, Spain, Jun. 2020, pp. 1–6, doi: 10.1109/EEEIC/ICPSEurope49358.2020.9160584.
- [19] M. Montani et al., 'ESC on In-Wheel Motors Driven Electric Vehicle: Handling and Stability Performances Assessment,' 2020 IEEE International Conference on Environment and Electrical Engineering and 2020 IEEE Industrial and Commercial Power Systems Europe (EEEIC / ICPS Europe), Madrid, Spain, 2020, pp. 1–6, doi: 10.1109/EEEIC/ICPSEurope49358.2020.9160768.
- [20] J. Jin, 'Modified Pseudoinverse Redistribution Methods for Redundant Controls Allocation', *Journal of Guidance, Control, and Dynamics*, vol. 28, no. 5, pp. 1076–1079, Sep. 2005, doi: 10.2514/1.14992.
- [21] H. Pacejka, *Tire and Vehicle Dynamics*. Elsevier, 2005.
- [22] T. Novi, R. Capitani, C. Annicchiarico, 'An integrated ANN-UKF vehicle sideslip angle estimation based on IMU measurements', in *Proceedings of the Institution of Mechanical Engineers, Part D: Journal of Automobile Engineering*, 233(7), pp. 1864–1878, 2016.
- [23] P. Falcone, H. Eric Tseng, F. Borrelli, J. Asgari, D. Hrovat, 'MPC-based yaw and lateral stabilisation via active front steering and braking', in *Vehicle System Dynamics* 46, pp. 611–628, 2008.
- [24] M. Guiggiani, *The science of vehicle dynamics: handling, braking, and ride of road and race cars*. Dodrecht: Springer, 2014.
- [25] E. Mosca, 'Optimal Predictive and Adaptive Control', in *Prentice Hall information and system sciences series*, Englewood Cliffs, 1995.
- [26] International Organization for Standardization, 'ISO 21994:2007-Passenger cars—Stopping distance at straight-line braking with ABS — Open-loop test method'.
- [27] International Organization for Standardization, 'ISO3888-1:1999-Passenger Cars-Test Track for a Severe Lane-change Manoeuvre: Part 1: Double Lane-change'.
- [28] International Organization for Standardization, 'ISO 19365:2016-Passenger cars — Validation of vehicle dynamic simulation — Sine with dwell stability control testing'.